Desalination and Water Treatment
www.deswater.com
doi: 10.1080/19443994.2013.827300

52 (2014) 805–815
January

Taylor & Francis
Taylor & Francis Group

Reactivity of different cement minerals in presence of Fe(II) for reducing trichloroethylene

Praveen A. Ghorpade, Jung-Hwan Kim, Won-Ho Choi, Joo-Yang Park*

Department of Civil and Environmental Engineering, Hanyang University, 17 Haengdang-dong, Seongdong-gu, Seoul, Korea
Tel. +82 2 2220 0411; Fax: +82 2 2220 1945; email: jooypark@hanyang.ac.kr

Received 19 March 2013; Accepted 6 May 2013

ABSTRACT

Ferrous iron Fe(II) in combination with Portland cement is effective in dechlorinating trichloroethylene (TCE). However, there is no clear evidence about the component in cement responsible for TCE dechlorination. In present study different cement hydration minerals, such as ettringite (AFt) and monosulfate (AFm) were synthesized separately in laboratory. The TCE dechlorination ability of these minerals in combination with Fe(II) was investigated. It was found that these minerals in pure form do not have TCE dechlorination capacity. Further α-hematite (α-Fe_2O_3) that is suspected reactive mineral in cement/Fe(II) was investigated. It was found that when extra pure α-Fe_2O_3 along with CaO/Fe(II) was used for TCE did not show any reduction potential. This result was contradictory to earlier researchers, who used α-Fe_2O_3/CaO/Fe(II) for dechlorination of TCE. Thus, the α-Fe_2O_3 (Bayferrox-110 M) used by earlier researchers was investigated and it was found that it had some other impurities present in it. These impurities were suspected to play significant role in dechlorination of TCE. Further detailed studies were carried out and α-Fe_2O_3 was synthesized by following manufacturing procedure given for α-Fe_2O_3 (Bayferrox-110 M). When such α-Fe_2O_3 was used for TCE reduction, it showed improved reactivity. Detailed investigations showed that the α-Fe_2O_3 not in pure form but in combination with other impurities has reduction capacity for TCE.

Keywords: TCE; Ettringite; Monosulfate; α-Fe_2O_3; Reduction

1. Introduction

Chlorinated ethylene and their adverse effects on environment have been studied by many researchers [1–3]. The iron based solidification and stabilization technology is one of the most popular technologies to remediate the ground water polluted with chlorinated solvents. This technology helps not only in immobilizing the organic and inorganic contaminants and prevent their spreading in surrounding environment, but also can degrade chlorinated hydrocarbons by reductive dechlorination [4,5].

*Corresponding author.

Presented at the Fifth Annual International Conference on "Challenges in Environmental Science & Engineering—CESE 2012" Melbourne, Australia, 9–13 September 2012

Previous studies showed that cement/Fe(II) based system can reduce chlorinated compounds, such as trichloroethylene (TCE) to harmless products like ethylene, ethane [4–6]. However, when mixing with water, the hydration of the cement leads to many complex phases. During the reaction different phases of cement such as alite, belite, aluminate, and ferrite, react with calcium sulfate leading to much complicated products like ettringite (AFt) and monosulfate (AFm) phases [7].

However, so far it has not been possible to identify specific mineral or mineral phase responsible for TCE dechlorination due to complexity of cement hydration minerals. It was [4] postulated that some of the cement hydration phases associated with elements such as Al^{3+} and Fe^{3+} and SO_4^{2-} could be responsible for TCE dechlorination. Ko and B. Batchelor [8], showed the presence of Fe^{3+} that was associated with hexagonal particles in samples of Portland cement slurry analyzed at the end of tetrachloroethylene reduction reaction. The hexagonal shape is characteristic shape of AFm phases in cement hydration. The hydration phases were composed of calcium, aluminum, and iron hydroxide [8]. It was suspected that AFm phases were the likely agents for PCE degradation [8].

Ettringite and monosulfate have been shown as one of the important cement hydration phases for the immobilization of many hazardous and heavy metals [9,10]. The Ettringite crystals have hexagonal rods with channel like morphology [11]. The Ettringite has general formula of $C_6(A,F)X_3H_y$, where ($C = CaO$, $A = Al_2O_3$, $F = Fe_2O_3$, $H = H_2O$) and X represents doubly or singly charged anion [7]. On the other hand AFm forms lamellar structure or layered double hydroxides with hexagonal shape with general formula of $C_4(A,F)X_2H_y$ [7]. The Al-ettringite (AFt) ($Ca_6(Al(OH)_6)_2(SO_4)_3{\cdot}26H_2O$), gets formed at the early hydration phases of cement, when aluminate phases (C_3A) react with calcium sulfate and water [7,12]. As the gypsum in the ettringite gets consumed hydrocalumite will get formed with which ettringite further reacts to give calcium monosulfoaluminate hydrate ($Ca_4Al_2O_6(SO_4){\cdot}12H_2O$) or Al-monosulfate (AFm) [7,12]. The cation substitutions in the crystal structures of both AFt and AFm have been reported by many researchers. Portland cement has 5–15% ferrite phase. It is reported by many researchers that in Portland cement Fe^{3+} partly replace Al^{3+} in the lattice structure of ettringite or monosulfate [13]. There is strong possibility of co-existence of Fe-ettringite and Fe-monosulfate along with Al-ettringite and Al-monosulfate in cement system. It was recently suggested that some of Al-Fe-mono (AFm) phases could be most likely reactive species in cement/Fe(II) system [8]. Another possibility was that reductive dechlorination occurs at the solid surfaces of minerals formed during cement hydration reaction [14]. Thus, it is important to study the different mineral phases formed during cement hydration. As the hydration products in combination with Fe(II) produce compounds responsible for TCE dechlorination [8]. Cement has Fe^{3+} originating from Fe_2O_3, however, it will be present in combined form of tetracalcium alumino ferrite ($4CaO\ Al_2O_3\ Fe_2O_3$). When Fe(II) is added to the cement system it is likely to react with Fe_2O_3 individually or other minerals in combination with Fe_2O_3 [15]. Previous study [16] compared TCE dechlorination rates of hematite/Fe(II) system with cement/Fe(II) system, however, the reactive solids analyzed at the end of the reaction were suspected to be green rust. Also, the reactivity was slightly different compared with that of cement/Fe(II) system [16]. Considering all above facts different AFt, AFm phases associated with Fe^{3+} and Al^{3+}, and minerals like Fe_2O_3 which are integral part of cement are suspected responsible candidates for dechlorination reactions in cement/Fe(II) system. The cement hydration reaction is quite complicated, and is composed of mixture of all these mineral phases. It is important to identify dechlorination capacity of individual mineral for better understanding of the reactivity of cement/Fe(II).

The objective of the present study was to synthesize different cement minerals such as ettringite and monosulfate associate with Al^{3+} and Fe^{3+} and evaluate their TCE dechlorination capacity in combination with Fe(II). In second phase of experimentation, the dechlorination ability of α-Fe_2O_3 that is another suspected mineral in cement was analyzed. For this study pure α-Fe_2O_3 and α-Fe_2O_3 made from pure iron powder and impure iron powder containing other elements as starting material were selected. To achieve these objectives, different cement minerals mentioned above were synthesized separately in laboratory by following the procedures given by various researchers with some modifications. The synthesized mineral phases were characterized using scanning electron microscope with energy dispersive spectroscopy (SEM-EDS) and X-ray diffraction (XRD). Further, the TCE dechlorinating capacities of individual mineral was examined in batch slurry experiments.

2. Materials and methods

2.1. Chemicals

The chemicals used were TCE (99.5%, Aldrich Chemical), 1,1-dichloroethylene (1,1-DCE, 99%, Aldrich Chemical), *cis*-dichloroethylene (*cis*-DCE, 97%, Aldrich

Chemical), *trans*-dichloroethylene (*trans*-DCE, 98%, Aldrich Chemical), vinyl chloride (VC, 2.0 mg/mL in methanol, Ac-cu Standard), 1% acetylene in nitrogen (Matheson Tri-Gas), 1,000 ppm ethylene in helium (Matheson Tri-Gas), 1,000 ppm ethane in helium (Matheson Tri-Gas), methanol (99.9%, HPLC grade, Fisher Scientific), hexane (99% HPLC grade), nitrobenzene (99.5%, Junsei Chemicals), acetone (99.5%, Aldrich Chemicals), ferrous sulfate (99.5%, heptahydrate, Acros Organics), ferric sulfate (97%, Aldrich Chemicals), calcium oxide (Aldrich Chemicals), calcium carbonate (99%, Sigma–Aldrich), calcium sulfate dihydrate (99%, Sigma–Aldrich), aluminum hydroxide (99%, Sigma–Aldrich), potassium hydroxide (Duksan pure chemicals), sodium hydroxide (Extra pure Duksan pure chemicals) aluminum chloride (Daejung, extra pure reagent), ferrous chloride (Daejung, extra pure reagent), sulfuric acid (extra pure, Duksan Pure Chemicals), α-Fe_2O_3 (99.9%, α-Fe_2O_3, High Purity Chemicals, Japan), iron powder (Showa Chemicals, 300 mesh), and extra pure iron powder (99.5%, Merck, 10 μm). Methalonic stock solutions of TCE were prepared daily. Stock solution of Fe(II) was prepared daily by dissolving the appropriate amount of ferrous sulfate in Milli-Q water.

2.2.2. Synthesis of different minerals

Different minerals namely Al-ettringite ($Ca_6(Al(OH)_6)_2(SO_4)_3{\cdot}26H_2O$), Al-monosulfate ($Ca_4Al_2O_6(SO_4){\cdot}12H_2O$), Fe-ettringite ($Ca_6Fe_2(SO_4)_3(OH){\cdot}12H_2O$), and Fe-monosulfate ($Ca_4Fe_2O_6(SO_4){\cdot}16H_2O$) were synthesized using the methods described by different researchers. α-Fe_2O_3 pure mineral used was supplied by 99.9% high purity chemicals, Japan. α-Fe_2O_3 from pure iron powder and iron powder containing other elements was made by following United States patent information and α-Fe_2O_3 (Bayferrox 110 M) product details. The synthesis details of all minerals are discussed as follows.

2.2.1. Synthesis of Al-ettringite

The Al-ettringite was synthesized by reaction of tricalcium aluminate (C_3A) and gypsum in presence of water. Initially, C_3A was made by mixing the molar proportions (3:2) of $CaCO_3$ and $Al(OH)_3{\cdot}xH_2O$. Two powders were mixed properly and the homogeneous mixture was heated at 1300˚C using an electric furnace for 72 h, with intermediate grinding at 24 h to ensure the homogeneity [17]. Thus, formed C_3A was mixed with gypsum in 1:1.2 M ratio (excess moles of $CaSO_4{\cdot}2H_2O$ compared to that of C_3A), which increases the chances of formation of ettringite structure because of more sulfate ion concentrations [18]. Water was added to carryout hydration reaction. The water to solid ratio was maintained at 10. All the reactions were carried out in closed polythene bottle in nitrogen atmosphere to avoid the CO_2 contamination. The entire mixture was heated at a temperature less than 60˚C with constant magnetic stirring for 36 h. Although the ettringite formation takes place in few hours [7], the heating was carried out so that the rate of hydration reaction increases and ettringite can get formed in lesser time than usual hydration time. Heating helps to accelerate the hydration reaction [17]. The temperature below 60˚C ensures that the formed AFt crystals are not destroyed, because above 70˚C the ettringite are not stable and get converted to monosulfate [19,20]. The reaction mixture was cooled using ice bath so that the crystal generation gets accelerated. The reaction mixture was filtered using Whatman filter No. 2 under vacuum. The filtered solids were washed with acetone to stop the hydration reaction [17]. The entire operation was carried under N_2 atmosphere. Thus, obtained solids were dried at room temperature in nitrogen environment.

2.2.2. Synthesis of Al-monosulfate

The synthesis of Al-monosulfate was the same as that of Al-ettringite. The only difference was that the ratio of C_3A: $CaSO_4{\cdot}2H_2O$ was 1:1 and the mixture was heated at elevated temperature range of 80 to 90˚C for 36 h. It is reported that ettringite crystals are not stable above temperature of 70˚C and get converted to monosulfate. But monosulfate crystals can exists even at 100˚C [19–21]. The gypsum proportion was also reduced so that sulfate was in less quantity. Deficit sulfate ion concentration favors the formation of monosulfate directly rather than forming ettringite [18]. In usual cement hydration reactions formation of monosulfate at 25˚C takes 8–11 days [22].

2.2.3. Synthesis of Fe-ettringite

The synthesis of Fe-ettringite was carried out by following the method described by Göril Möschner [23]. Fe-ettringite was synthesized by addition of 0.039 mol/L of $Fe_2(SO_4)_3{\cdot}5.3H_2O$ and 0.229 mol/L freshly prepared CaO to 0.016 M KOH at a liquid/solid ratio of 20.The mixing was carried out in gloved box to avoid CO_2 contamination. In original experiment the time dependence of formation of ettringite was observed on 7, 24, 45, 90, and 180 days. In our case, we took the ettringite crystals formed at the end of the 7 days. The solids precipitated were separated

by a vacuum filtration and were dried at room temperature in nitrogen chamber. The rate of formation of Fe-ettringite is much slower compared to the formation of the Al-ettringite [24].

2.2.4. Synthesis of Fe-monosulfate

To make Fe-monosulfate, initially calcium ferrite ($Ca_2Fe_2O_5$) was synthesized by mixing calcium carbonate and hematite (Fe_2O_3) in 2:1 M ratio. The mixture was properly mixed and heated at 1,000˚C for 2 h [25]. Thus, formed $Ca_2Fe_2O_5$ was then mixed with $CaSO_4{\cdot}2H_2O$ (1:1.5) and hydration reaction was carried with the water to solid ratio of 10. The mixture was heated at 80˚C for 36 h. The entire reaction was carried out in high density polythene bottle with closed lid under N_2 atmosphere. The reaction products were similar to that of reaction of C_3A and gypsum. The only difference was instead Al-monosulfate the product formed was Fe-monosulfate.

2.2.5. Synthesis of α-Fe_2O_3 from pure iron powder and impure iron powder

Initially, the extra pure α-Fe_2O_3 (99.9% high purity chemicals, Japan) was used for TCE experiments. When it did not show reduction capacity for TCE, the synthesis of α-Fe_2O_3 was carried out by following the manufacturing details of α-Fe_2O_3 (Bayferrox 110 M that was used by earlier researchers) given in the US patent [26,27] and Bayferrox product manual [28]. Two different types of α-Fe_2O_3 were synthesized by using pure iron powder and iron powder containing different elements as a starting material, respectively.

Initially, the extra pure iron powder (supplied by Merck) was mixed with nitrobenzene, this reaction reduces nitrobenzene to aniline and iron powder gets oxidized to iron oxide black (Fe_3O_4). Further, this black powder of Fe_3O_4 was calcined at 800˚C to get pure α-Fe_2O_3. Similar procedure was repeated for impure iron powder (supplied by Showa chemicals 300 mesh size) containing other elements in it to get α-Fe_2O_3 with other elements.

2.3. Experimental procedure for TCE

All the experiments were carried out in clear borosilicate glass vials (23.4 ± 0.13 mL) with triple seals that were designed to reduce the intrusion of oxygen and volatilization of TCE. All the samples were prepared in an atmospheric environment at ambient temperature (22 ± 0.5˚C). The reactive samples were prepared either in duplicate or in triplicate. The controls were made by deionized water and TCE. The slurry samples were prepared by appropriate mineral solids and appropriate aliquots of water and Fe(II) stock solution of 100 mM for AFt and AFm minerals. For hematite experiments, the slurry samples were prepared by appropriate solids (CaO + α-Fe_2O_3, 4:1 mol ratio) and appropriate aliquots of water and Fe(II) stock solution of 200 mM. The mass ratio of solids to solution was 0.10. The vials were filled completely with the aqueous solutions so as to minimize gas phase partitioning of the chlorinated solvents. The CaO was added in hematite experiment in above mentioned mole ratio, so as to maintain the pH in the range of 12.3–12.5. As soon as the slurry reactors were made, 10 μL of methalonic stock solution of TCE was spiked in to the reactor, so as to get 32.8 mg/L (0.25 mM) of initial concentration of TCE. After TCE was spiked, the reactors were rapidly capped with closures and were placed on a rotary motion with end over end rotation of 8 rpm. At specified intervals of time the duplicate or triplicate samples were retrieved from the rotator and were centrifuged at 112 × g for 3 min to separate solids and aqueous phase. For TCE, 50 μL of aliquot was extracted with 1000 μL of hexane in a 2 mL GC vial. The vials were shaken for 5 min on an orbital shaker. After equilibrating at room temperature the samples were analyzed on GC. For gas (VC, ethylene, acetylene, ethane) analysis, approximately 10 mL of aqueous samples were rapidly transferred to 24 mL glass vials and were equilibrated with the gas phase of the vials to be prepared for headspace analysis.

2.4. Analytical methods

TCE, 1,1-DCE, *cis*-DCE, and *trans*-DCE were analyzed on gas chromatography (GC, Shimadzu GC-17A) equipped with an electron capture detector and a HP-5 column (30 m × 0.250 mm i.d × 0.25 μm film thickness; Agilent tech). Hexane extractant was injected in a split mode of (50:1) using an auto sampler at 250˚C. Extra pure nitrogen was used as a carrier gas at a flow rate of 1.5 mL/min. The oven temperature was isothermal at 60˚C for 3 min, ramped to 150˚C at a rate of 15˚C min^{-1} and held for 5 min. The temperature of the detector was 280˚C.

VC, acetylene, ethylene, and ethane were analyzed on GC (Younglin M600D) equipped with a flame ionization detector and a GS-Alumina column (50 m × 0.53 mm i.d.; J&W Scientific). Headspace samples were injected manually with a split ratio of 10:1 using a 100-μL gastight syringe. The oven temperature was held at 80˚C for 1 min, ramped to 100˚C at a rate of 5˚C min^{-1}, and held for 2 min. The injector and

detector temperatures were 250 and 320°C, respectively. Nitrogen was used as a carrier gas at a flow rate of 2.7 mL/min. Nonchlorinated gas products were calibrated using the gas standards mentioned above (Matheson Tri-Gas).

The synthesized mineral powder samples were analyzed using XRD analysis. Powder XRD with 2θ values ranging from 4 to 90° using a Bruker AXS D5005 goniometer were collected at a constant scanning rate of 1°C min^{-1} with CuKα radiation

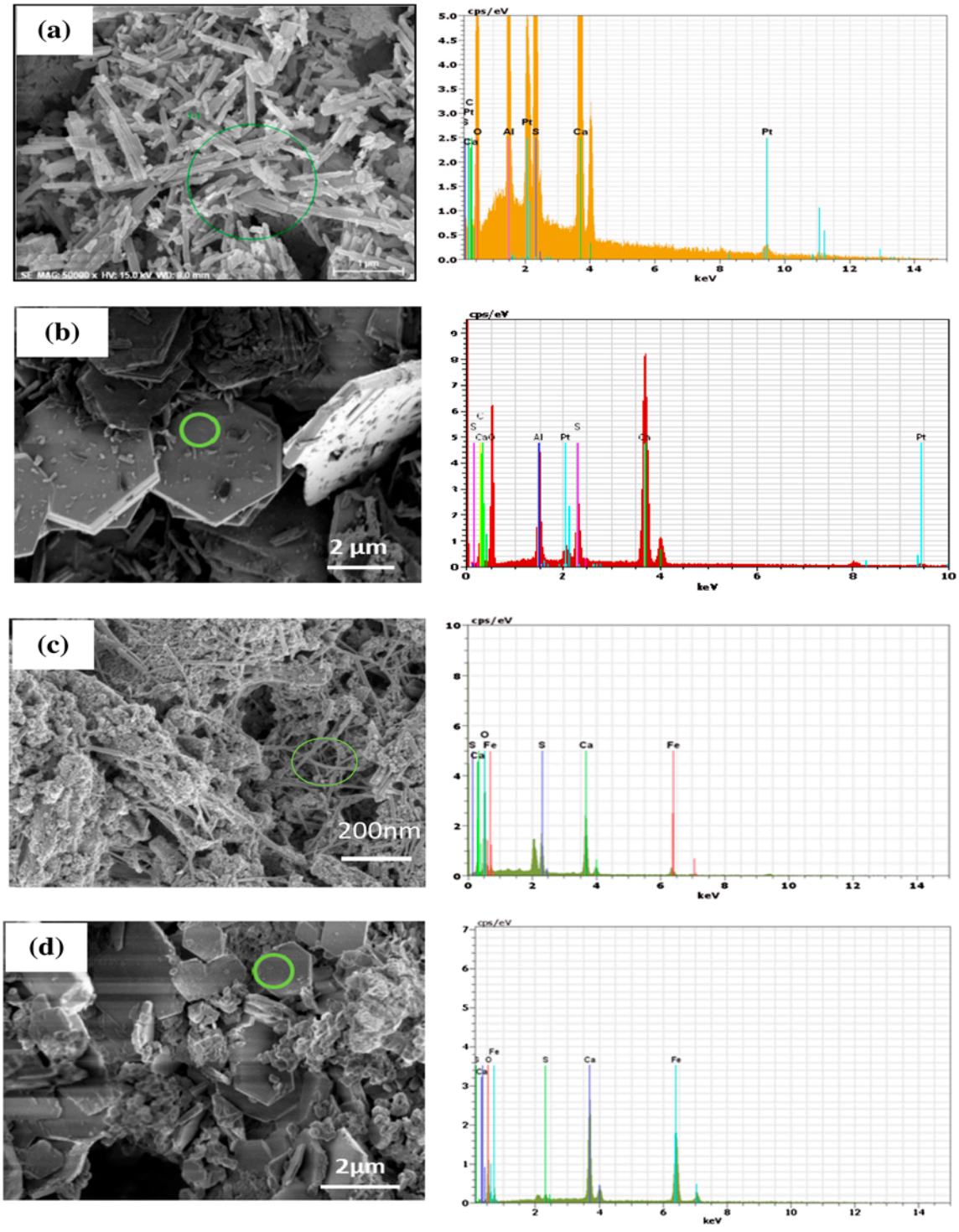

Fig. 1. SEM and EDS images of (a) Al-ettringite, (b) Al-monosulfate, (c) Fe-ettringite, and (d) Fe-monosulfate.

($\lambda = 1.540$ nm). The resultant peaks of individual minerals were compared with JCPDS cards. The surface morphologies of the solid minerals was carried out using field emission scanning electron microscope (Carl Zeiss SUPRA 55VP) with platinum coating by sputter coater (BAL-TEC/SCD 005). The quantitative measurements were performed on wavelength dispersive X-ray fluorescence spectrometer (WDXRF, Bruker AXS S4 PIONEER). The pH was measured with a pH meter (Orion 720A+) and electrode (9157BN).

2.5. Kinetic analysis

Pseudo-first-order rate law was used to describe the TCE reduction kinetics of hematite, CaO, and Fe(II) system. A generic pseudo-first-order equation is as shown below:

$$\frac{C}{C_o} = e^{-kt}$$

where C is final concentration of TCE in (mg/L) in aqueous phase at reaction time "t" (d^{-1}).

3. Results and discussion

3.1. Reactivity of different ettringite and monosulfate with TCE in presence of Fe(II)

Fig. 1 shows the SEM and EDS images of the synthesized AFm and AFt phases, Fig. 2 shows the XRD

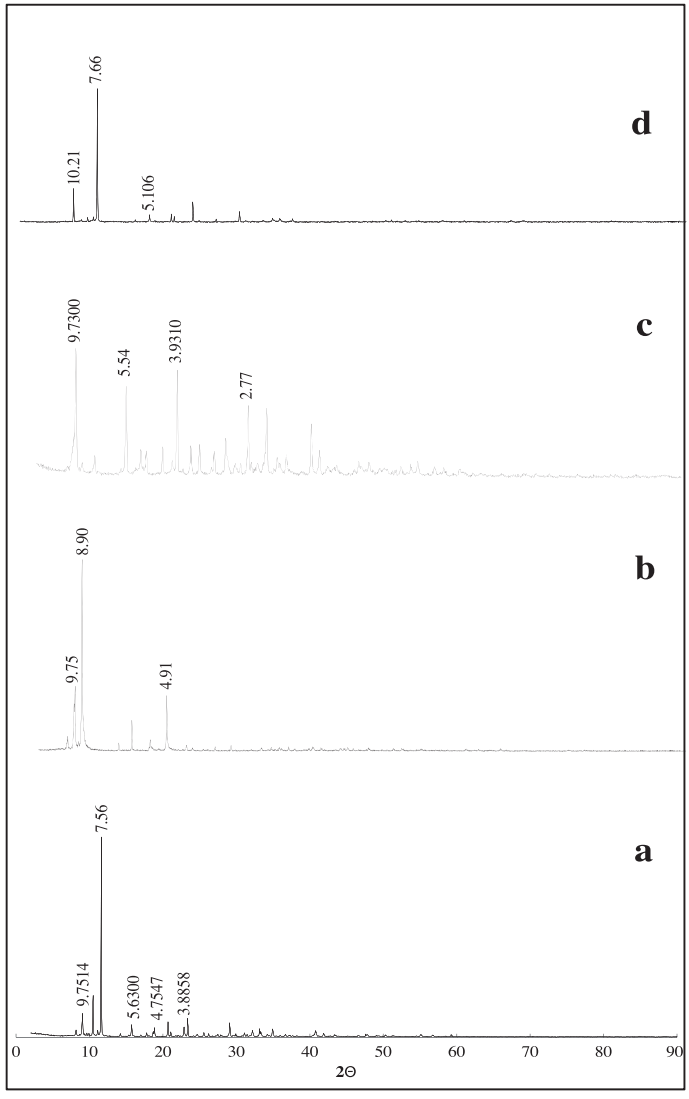

Fig. 2. XRD patterns of (a) Al-ettringite, (b) Al-monosulfate, (c) Fe-ettringite, and (d) Fe-monosulfate.

analysis of ettringite and monosulfate associated with Al^{3+} and Fe^{3+}. All the solids were dried in N_2 atmosphere before taking SEM and XRD. Fig. 1(a) shows the typical SEM and EDS image of the Al-ettringite, large number of rod like structure with uniform morphology were seen. The average particle size of the ettringite crystal was found to be (1.2 μm). The EDS spectra of the crystal surface showed the presence of Al, S, O, Ca elements which are representative elements of Al-ettringite. Fig. 2(a) shows the XRD analysis of Al-ettringite with d-spacing values at 9.75, 5.63, 4.75, and 3.88 Å. The peak values were compared with standard card of Al-ettringite (JCPDS card No. 720646). Strong peak was observed at 7.56 Å which was of unreacted tricalcium aluminate ($Ca_3Al_2O_6$) (JCPDS card No. 320150). Fig. 1(b) shows the hexagonal morphology of Al-monosulfate crystal, traces of ettringite rods were also seen in the SEM image, although hexagonal crystals were more dominant minerals. EDS elemental analysis showed the elemental composition of (Al, S, O, Ca). The elemental composition of monosulfate is same as that of ettringite, but the morphology is different so as the crystal size. The average crystal size of Al-monosulfate was found to be (19 μm) and thickness of (0.7 μm). The SO_4^- ions were more in Al-ettringite compared to Al-monosulfate. Further, XRD analysis was done to confirm the Al-monosulfate. As shown in Fig. 2(b) peaks positions at 8.90, 4.91 Å show strong peaks of Al-monosulfate (JCPDS card No. 450158). The peak at 7.56 Å which is representative peak of C_3A was not seen in the XRD. It shows that C_3A completely reacted to give major phase of Al-monosulfate. The peaks at 9.75 Å showed small amount of Al-ettringite (JCPDS card No. 720646). Further, Fe-ettringite which was made by the co precipitation method described above. The solids formed at the end of the 7 days were taken for the analysis. Fig. 1(c) shows the SEM image of Fe-ettringite. The morphology of crystals showed tiny network of rods. The rods were of Fe-ettringite, the crystal structure was not as clear as that of Al-ettringite because of the fact that the hydration reaction of Fe^{3+} are slower compared to that of Al^{3+} [24] and also the temperature was not enhanced, as it was done in other cases. The EDS data confirms the representative elemental composition of (Fe, S, O, Ca). The average crystal size was (1 μm).The XRD of Fe-ettringite is as shown in Fig. 2(c) the strong peaks at 9.73, and 3.93 Å are of Fe-ettringite (JCPDS card No. 400292). Since this reaction was time dependent and formed Fe-ettringite at the end of 7 day was taken for experiments. Since the reaction was still undergoing the formation of ettringite crystals, the presence of unreacted calcium sulfate in the form of calcium sulfate hydrate was expected in the reaction mixture. The calcium sulfate hydrate peak was clearly seen in the XRD plot at peak position of 5.54 and 2.77 Å (JCPDS card No. 840962). Fig. 1(d) shows the SEM and EDS of Fe-monosulfate, the SEM image showed plate like crystals the crystal morphology was not as clear as that of Al-monosulfate although the reaction time was similar with the similar temperature conditions. It is reported that the ettringite and monosulfate formations with Fe^{3+} will take more time compared to Al^{3+}. The average crystal size was found to be (3.2 μm) and EDS spectra showed the presence of Fe along with Ca, S, O which are repetitive elements of Fe-monosulfate. Fig. 2(d) gives XRD of Fe-monosulfate peak at 10.21, 5.106 Å (JCPDS card No. 440605). The d spacing values and intensity in case of Fe-monosulfate was slightly different as compared to standard card. This could be caused,

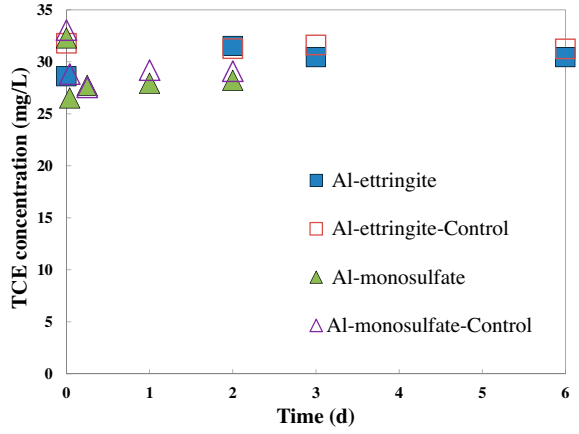

Fig. 3. TCE concentrations in presence of Al-ettringite and Al-monosulfate. The controls contain TCE and water.

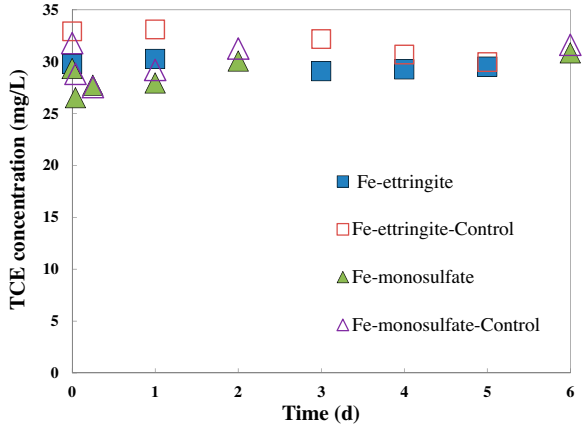

Fig. 4. TCE concentartions in presence of Fe-ettringite and Fe-monosulfate. The controls contain TCE and water.

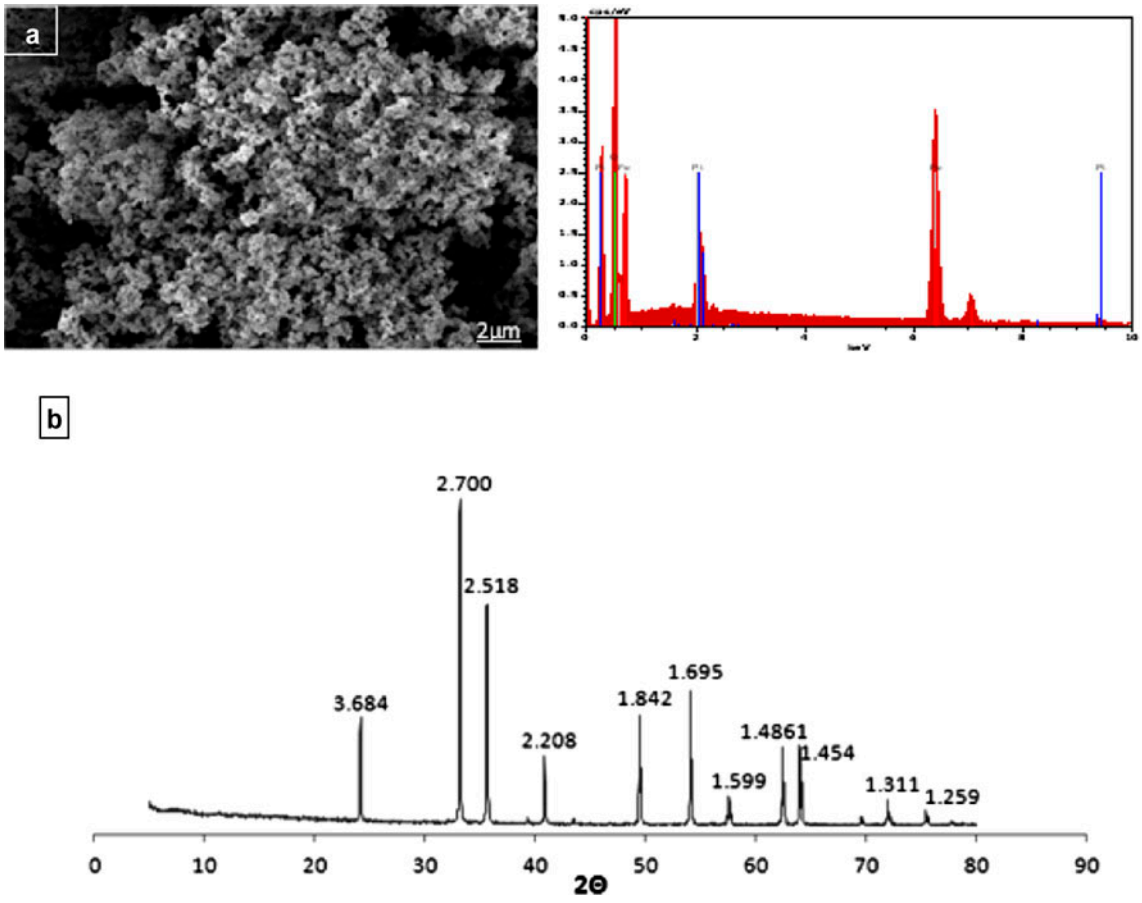

Fig. 5. (a) SEM and EDS spectra of pure α-Fe_2O_3 and (b) XRD patterns of pure α-Fe_2O_3.

because of different chemical compositions of solids used during the experiments to that of standards and also because of different reaction conditions. The strong peak at 7.66 Å was of unreacted calcium ferrite (JCPDS card No. 720891).

Further batch experiments were conducted to check the individual minerals ability to dechlorination TCE in presence of Fe(II). Figs. 3 and 4 shows the TCE behavior in Al ettringite, Al monosulfate and Fe-ettringite, Fe-monosulfate, respectively. It can be clearly seen that there was no considerable reduction in the TCE concentrations.

3.2. Reactivity of pure α-Fe_2O_3 and α-Fe_2O_3 prepared from pure iron powder and impure iron powder in presence of Fe(II) and CaO

Initially, the extra pure α-Fe_2O_3 (99.9% high purity chemicals, Japan) was chosen for TCE reduction experiments. Fig. 5(a) shows the SEM and EDS of the extra pure α-Fe_2O_3. The EDS spectra showed, the presence of only iron and oxygen and there was no other impurity present in the sample. Fig. 5(b) shows

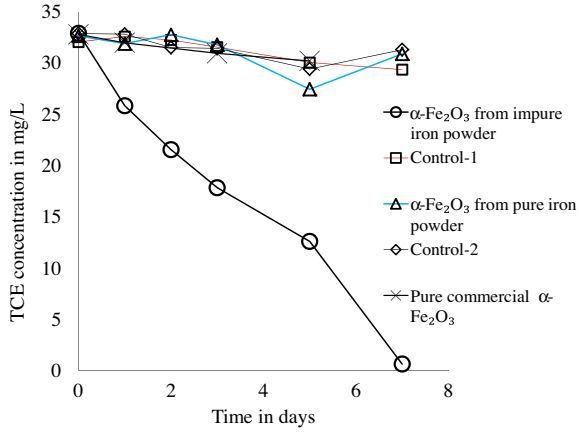

Fig. 6. Change in TCE concentration with different types of α-Fe_2O_3 systems.

XRD plot of pure α-Fe_2O_3. Peaks were found to have matched with JCPDS card No. 87–1166. The TCE experiments were carried out using this hematite with CaO and 200 mM of Fe(II). The samples were analyzed at 0, 1, 3, and 5 days. Fig. 6 shows the reactivity of pure α-Fe_2O_3. The results indicated that there was no reduction in TCE concentration even after 5 days of reaction. Since the pure hematite was not showing reduction capacity, the α-Fe_2O_3 used by previous researchers was analyzed using XRF. The analysis showed presence of many other elements in it. These elements were suspected to play significant role in TCE dechlorination reaction. Considering these facts different experiments of synthesizing the α-Fe_2O_3 by using pure iron powder and impure iron powder as starting material was planned. Thus, prepared different types of hematite were used for TCE reduction experiments. Table 1(a) shows the XRF analysis of α-Fe_2O_3 used by previous researchers (Bayferrox-110 M) and Table 1(b) shows XRF analysis of impure iron powder used as starting material to make α-Fe_2O_3 in our experiments. When the elements present in both the cases were compared they were almost identical, however, but their concentration was not the same. In our experiments two different types of hematite was synthesized using pure iron (99.5%, Merck, 10 μm), as starting material and impure iron (obtained from Showa) as staring material. By following the procedure discussed in section 2.2.5. Fig. 7(a) shows the XRD pattern of impure iron powder. Fig. 7(b) shows the α-Fe_2O_3 made from impure iron powder. Fig. 7(c) shows XRD of pure iron powder. When the *d* values were compared with that of impure iron powder, a slight shift in *d* values was seen. This could be because of impurities present in impure iron powder. Fig. 7(d) shows the XRD plot of α-Fe_2O_3 made from pure iron powder. The *d* values of this α-Fe_2O_3 were comparable with that of pure α-Fe_2O_3 hematite shown in Fig. 5(b).

Table 1
XRF analysis of (a) α-Fe_2O_3 (Bayferrox®-110 M) and (b) iron powder containing other elements

Elemental weight %	α-Fe_2O_3 (Bayferrox®–110 M)	Iron powder containing other elements (obtained from Showa) used for making α-Fe_2O_3
Mg	0.094	–
Al	0.081	0.16
Si	1.380	5.86
P	0.107	0.375
S	0.035	0.091
Ca	3.116	0.071
Cr	0.122	0.041
Mn	0.434	0.755
Fe	94.31	92.34
Ni	0.040	0.026
Cu	0.243	0.196
Zn	0.044	–
Nb	0.010	–
Mo	0.027	0.021
Ti	–	0.042

Results of the TCE reduction experiments with α-Fe_2O_3 made from impure iron powder as starting material and α-Fe_2O_3 made from pure iron powder are as shown in the Fig. 6. The α-Fe_2O_3 made from impure iron powder showed reduction capacity for

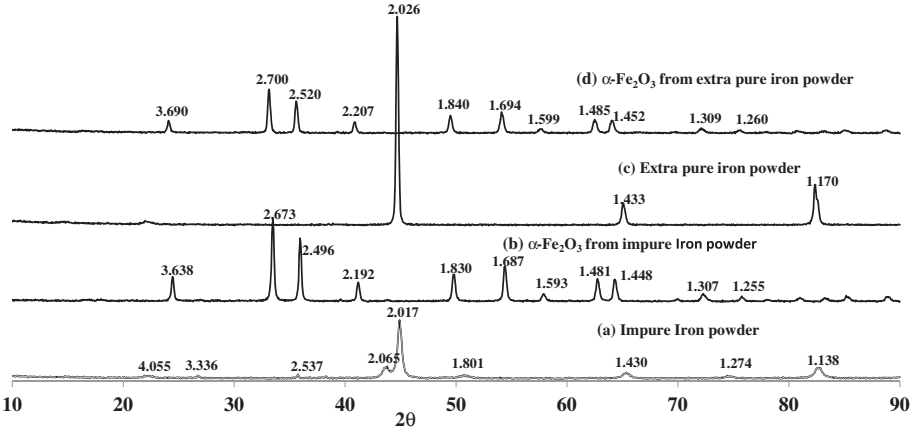

Fig. 7. XRD analysis of (a) impure Iron powder (obtained from Showa), (b) α-Fe_2O_3 from impure iron powder, (c) pure iron powder, and (d) α-Fe_2O_3 made from pure iron.

TCE. Impure α-Fe_2O_3 was able to reduce TCE concentrations to almost zero after 7 days. However, both the pure α-Fe_2O_3 and α-Fe_2O_3 made from pure iron powder do not show any reduction capacity for TCE.

The k value of the α-Fe_2O_3 from impure iron was found to be ($k = 0.2365\,d^{-1}$, $R^2 = 0.9328$) although it was not comparable with the earlier researchers Kim et al. [16] ($k = 0.57\,d^{-1}$) still our results show significance of other co-existing elements present in hematite made from impure iron source has a capacity to reduce TCE. The reason for change in the reactivity of α-Fe_2O_3 in present study and previous study could be because the iron powder used in both the cases was of different origin and so as the number of elements present in could vary in their concentration. We hypothesize that in case of α-Fe_2O_3 containing other elements the TCE dechlorination reactions must be taking place on the surface, and the bimetallic oxide system in α-Fe_2O_3 must be catalyzing the dechlorination reactions. Similar findings are reported by Choi et al. [29] and Cheng et al. [30].

3.3. Degradation products and end product analysis

During the experimentation with impure hematite/CaO/Fe(II) system the chlorinated degradation products like 1,1 DCE, *cis* and *trans*-DCE, and VC were not detected. The final degradation products were analyzed to get the information of pathway of dechlorination of TCE in hematite from impure iron powder experiment. The head space analysis of samples was done at the end of 7th day. The presence of ethylene, acetylene, and ethane was detected. In present study, we did not quantify the end products; we only detected them in the samples in which the TCE concentration was reduced to make sure that the TCE was reductively dechlorinated. The presence of acetylene shows the dechlorination was probably via β-elimination path way. The gas chromatogram (Fig. 8) indicates the presence of ethylene, acetylene, and ethane at retention time of 2.16, 2.31, and 2.60, respectively.

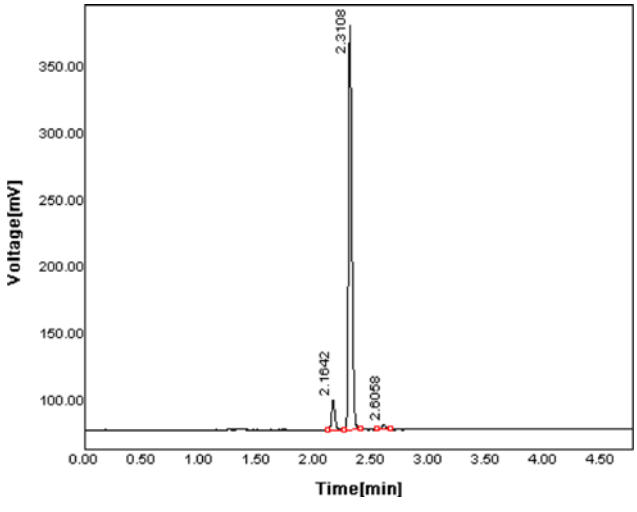

Fig. 8. The gas chromatogram shows the presence of ethylene, acetylene, and ethane at retention time of 2.16, 2.31, and 2.60, respectively, in a head space analysis of sample containing α-Fe_2O_3 from the iron powder containing other elements at the end of the 7th day.

4. Conclusions

We successfully synthesized pure mineral phases of monosulfate and ettringite associated with Al^{3+} and Fe^{3+}. The mineral were confirmed by SEM, EDS, and XRD analysis. The TCE dechlorination ability of individual mineral was in presence of Fe(II). Our studies indicated that these minerals individually in pure state do not show any capacity to reduce TCE. Further, the reactivity of pure and impure α-Fe_2O_3/CaO/Fe(II) was evaluated. The results indicated that extra pure α-Fe_2O_3 do not have capacity to reduce TCE. However, α-Fe_2O_3 which has other elements present in it was found to be efficient in reducing the TCE concentration. We suspect that in cement/Fe(II) system for dechlorination of TCE one single mineral in its pure state might not be responsible, but minerals in combination with other elements play significant role.

Acknowledgment

This study was supported by a National Research Foundation of Korea grant funded by the Korean government (MEST) (No. 2009-0086484).

References

[1] D. Henschler, G. Bonse, H. Greim, Carcinogenic potential of chlorinated ethylenes, tentative molecular rules, IARC Sci. Publ. 13 (1976) 171–175.
[2] L. Rhomberg, Dose response analyses of the carcinogenic effects of trichloroethylene in experimental animals, Environ. Health Perspect.108 (2000) 343–358.
[3] M. Fuller, K. Scow, Impact of trichloroethylene and toluene on nitrogen cycling in soil, Appl. Environ. Microbiol. 63 (1997) 4015–4019.
[4] I. Hwang, B. Batchelor, Reductive dechlorination of tetrachloroethylene by Fe(II) in cement slurries, Environ. Sci. Technol. 34 (2000) 5017–5022.
[5] I. Hwang, H.J. Park, W.H. Kang, J.Y. Park, Reactivity of Fe (II)/cement systems in dechlorinating chlorinated ethylenes, J. Hazard. Mater. B118 (2005) 103–111.
[6] B. Jung, B. Batchelor, Analysis of chlorination kinetics of chlorinated aliphatic hydrocarbon by Fe(II) in cement slurries, J. Hazard. Mater. 152 (2008) 62–70.
[7] H.F.W. Taylor, Cement Chemistry, Thomas Telford Services Ltd, London, 1997.

[8] S. Ko, B. Batchelor, Identification of active agents for tetrachloroethyelene degradation in Portland cement slurry containing ferrous iron, Environ. Sci. Technol. 41 (2007) 5824–5832.
[9] V. Albino, R. Cioffi, M. Marroccoli, L. Santoro, Potential application of ettringite generating systems for hazardous waste stabilization, J. Hazard. Mater. 51 (1996) 241–252.
[10] G. Sposito, Chemical Equilibria and Kinetics in Soils, Oxford Univ. Press, New York, 1994.
[11] A.W. Moore, H.F.W. Taylor, Crystal structure of ettringite, Acta Crystallogr. B Struct. Sci. 26 (1970) 386–393.
[12] E.M. Gartner, J.F. Young, D.A. Damidot, I. Jawed, J. Bensted, P. Barnes, Structure and Performance of Cement, Spon press, London, 2002.
[13] N. Meller, C. Hall, A.C. Jupe, S.L. Colston, S.D.M. Jacques, P. Barens, J. Phipps, The paste hydration of brownmillerite with and without gypsum: A time resolved synchrotron diffraction study at 30, 70, 100 and 150°C, J. Mater. Chem. 14 (2004) 428–435.
[14] J. Klausen, S.P. Trüber, S.B. Haderlein, R.P. Schwarzenbach, A reduction of substituted nitrobenzenes by Fe(II) in aqueous mineral suspensions, Environ. Sci. Technol. 29(9) (1995) 2396–2404.
[15] M. Elsner, R. Schwarzenbach, S. Haderlein, Reactivity of Fe (II)–bearing minerals toward reductive transformation of organic contaminants, Environ. Sci. Technol. 38 (2004) 799–807.
[16] H.S. Kim, W.H. Kang, M. Kim, J.Y. Park, I. Hwang, Comparison of hematite/Fe(II) systems with cement/Fe(II) systems in reductively dechlorinating trichloroethylene, Chemosphere 73 (2008) 813–819.
[17] B.A. Clark, P.W. Brown, The formation of calcium sulfoaluminate hydrate compounds part I, Cem. Concr. Res. 29 (1999) 1943–1948.
[18] A.N. Christensen, T.R. Jensen, J.C. Hanson, Formation of ettringite, $Ca_6Al_2(SO_4)_3$ $(OH)_{12}\cdot 26H_2O$, AFt, and monosulfate, $Ca_4Al_2O_6(SO_4)\cdot 14H_2O$, AFm-14, in hydrothermal hydration of Portland cement and calcium aluminum oxide-calcium sulfate dehydrate mixtures studied by *in situ* synchrotron X-ray powder diffraction, J. Solid State Chem. 177 (2004) 1944–1951.
[19] H.F.W. Taylor, C. Famy, K.L. Scrivener, Delayed ettringite formation, Cem. Concr. Res. 31 (2001) 683–693.
[20] C. Famy, K.L. Scrivener, H.F.W. Taylor, J. Bensted, P. Barnes (Eds), Structure and Performance of Cements, Spon Press, London, 2002, pp. 282–284.
[21] C. Hall, P. Barnes, A.D. Billimore, A.C. Jupe, X. Turrillas, Thermal decomposition of ettringite $Ca_6[Al(OH)_6]_2(SO_4)_3$ $26H_2O$, J. Chem. Soc., Faraday Trans. 92 (1996) 2125–2129.
[22] P.W. Brown, Kinetics of tricalcium aluminate and tetracalcium aluminoferrite hydration in the presence of calcium sulfate, J. Am. Ceram. Soc. 76(12) (1993) 2971–2976.
[23] G. Möschner, B. Lothenbach, J. Rose, A. Ulrich, R. Figi, R. Kretzschmar, Solubility of Fe-ettringite (Ca_6 [Fe $(OH)_6]_2(SO_4)_3\cdot 26H_2O$), Geochim. Cosmochim. Acta 72 (2008) 1–18.
[24] R.B. Perkins, C.D. Palmer, Solubility of (Ca_6 [Al $(OH)_6]_2(SO_4)_3\cdot 26H_2O$) at 5–75°C, Geochim. Cosmochim. Acta 63 (1999) 1969–1980.
[25] J.W. Jeon, S.M. Jung, Y. Sasaki, Formation of calcium ferrites under controlled oxygen potentials at 1273 K, ISIJ Int. 50 (2010) 1064–1070.
[26] B. Kröckert, G. Buxbaum, A. Westerhaus, Heat Stable Iron Oxide Pigments of Upsilon-Fe_2O_3 Structure, A Process for their Production and their Uses, United States Patent 5049193, 1991.
[27] H. Brunn, H. Bade, F. Hund, Process for the Production of Iron Oxide Red Pigments, United States Patent 4234348, 1980.
[28] LanXess Energizing Chemistry, Product information Bayferrox®-110M, LANXESS Deutschland GmbH Business Unit, Inorganic Pigments, D-51369 Leverkusen, 2009.
[29] J. Choi, B. Batchelor, J. Chung, Reductive dechlorination of tetrachloroethylene by green rusts modified with copper, Water Air Soil Pollut. 212 (2010) 407–417.
[30] I.F. Cheng, Q. Fearnando, N. Korte, Elcetrochemical dechlorination of 4-chlorophenol to phenol, Environ. Sci. Technol. 31 (1997) 1074–1078.